Volume 56
Number 2
7 January 2020
Pages 167–322

ChemComm

Chemical Communications

rsc.li/chemcomm

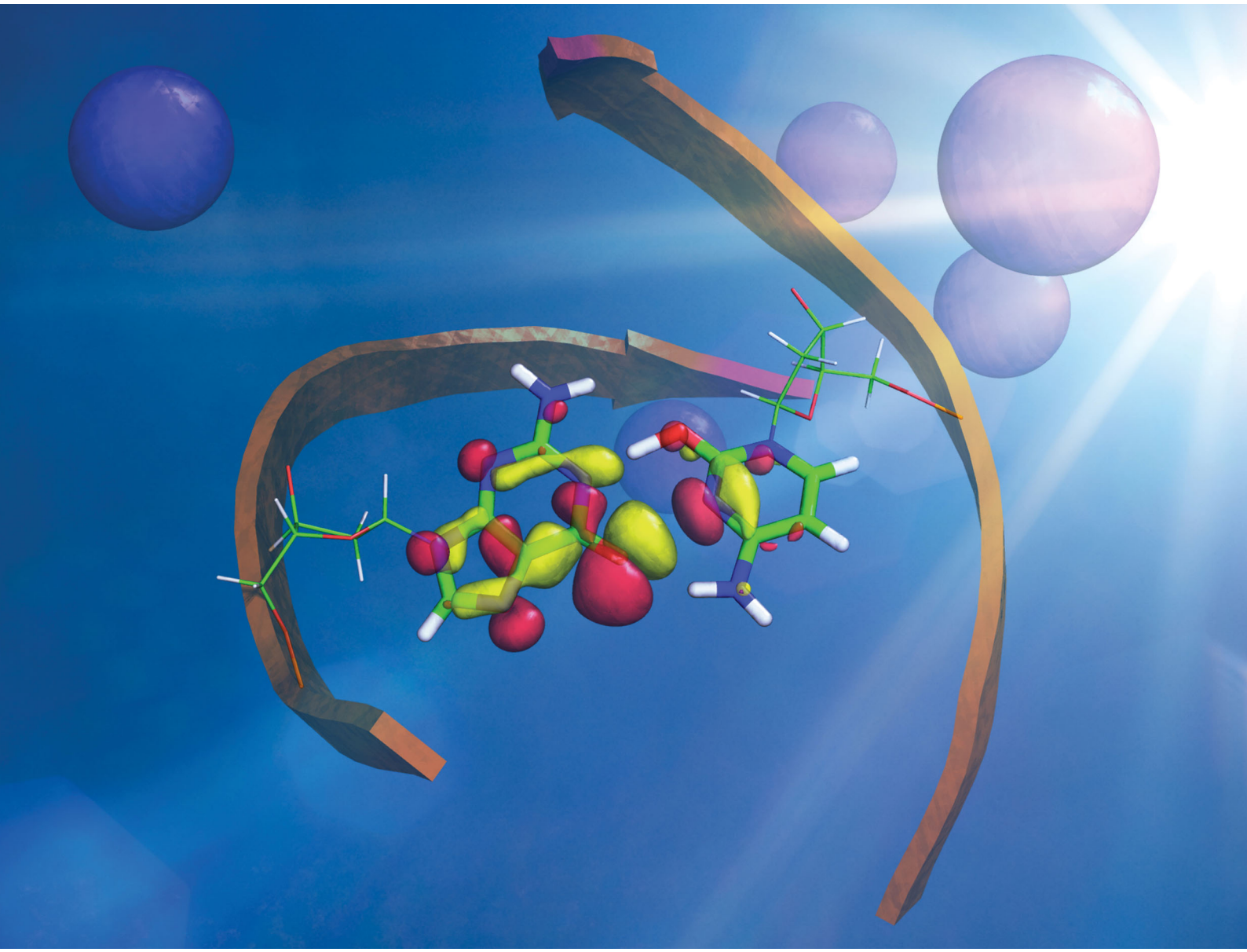

ISSN 1359-7345

ROYAL SOCIETY OF CHEMISTRY

COMMUNICATION

Robert W. Góra, Rafał Szabla *et al.*

UV-induced hydrogen transfer in DNA base pairs promoted by dark nπ* states

ChemComm

COMMUNICATION

View Article Online
View Journal | View Issue

Cite this: *Chem. Commun.*, 2020, **56**, 201

Received 9th August 2019,
Accepted 17th October 2019

DOI: 10.1039/c9cc06180k

rsc.li/chemcomm

UV-induced hydrogen transfer in DNA base pairs promoted by dark nπ* states†

Kinga E. Szkaradek,[a] Petr Stadlbauer,[bc] Jiří Šponer,[bc] Robert W. Góra *[a] and Rafał Szabla *[cd]

Dark nπ* states were shown to have substantial contribution to the destructive photochemistry of pyrimidine nucleobases. Based on quantum-chemical calculations, we demonstrate that the characteristic hydrogen bonding pattern of the GC base pair could facilitate the formation of a wobble excited-state charge-transfer $n\pi^*_{CT}$ complex. This entails a barrierless electron-driven proton transfer (EDPT) process which enables damageless photodeactivation of the base pair. These photostabilizing properties are retained even when guanine is exchanged to hypoxanthine. The inaccessibility of this process in the AT base pair sheds further light on the reasons why cytosine is less susceptible to the formation of photodimers in double-stranded DNA.

Photoinduced electron transfer is a ubiquitous phenomenon that could trigger various photochemical reactions, regulates the efficiency of organic solar cells and contributes to the photophysics and repair of DNA.[1] Such charge migration in biomolecules often entails a proton transfer and subsequent efficient photodeactivation through a crossing between the S_1 and S_0 states.[2] This process is often referred to as electron-driven proton transfer (EDPT)[3] or sequential proton-coupled electron transfer (PCET)[4] and was suggested as an origin of short excited-state lifetimes and photostability of the key biomolecular building blocks[5] and microsolvated organic chromophores.[6] One of the most representative examples of EDPT was reported for the Watson–Crick (WC) guanine–cytosine (**GC**) base pair in the gas phase, based on pump–probe spectroscopic measurements and quantum chemical calculations.[7] These findings enabled to assign the accessibility of the EDPT mechanism in WC base pairs to the presence of low-energy $^1\pi\pi^*_{CT}$ charge-transfer (CT) states, involving electronic transitions between bonding π molecular orbital localized on guanine and antibonding π* orbital localized on cytosine (*cf.* Fig. 2). More recent studies demonstrated that EDPT could also contribute to the photostability of **GC** in solution and in the native environment of DNA double helix.[8]

In opposition to the photostabilizing EDPT mechanism, pyrimidine nucleosides were shown to follow a competing photodeactivation pathway associated with the population of locally excited (LE) $^1n\pi^*$ states with lifetimes exceeding tens of ps.[9] These dark states could further serve as a doorway to even longer-lived and highly-reactive triplet $^3\pi\pi^*$ electronic states[10] enabling dimerization of adjacent pyrimidine bases.[11] The $^1n_O\pi^*$ state accessed after photoexcitation of cytidine was also demonstrated to enable abstraction of the C1′–H hydrogen atom from the sugar moiety and subsequent photoanomerisation from the naturally occurring β to the α anomer.[12] Finally, $^1n\pi^*$ states were suggested to participate in a water-splitting reaction in which the nucleobase abstracts a hydrogen atom from the neighboring water molecule and generates a hydroxyl radical.[13] The $^\bullet$OH radical could further attack the hydrogenated chromophore radical leading to the formation of a photohydrate, yet another type of photolesion that could significantly impede the functions of DNA and RNA.[13]

Despite similar contribution of $^1n\pi^*$ states to the photodynamics of the three canonical pyrimidine RNA/DNA bases,[9] cytosine was found to be the least susceptible to form photolesions in nucleic acid strands.[14] Therefore, our working hypothesis is that the lowest-energy $^1n\pi^*$ state of cytosine might promote an efficient photorelaxation channel which is unavailable in the **AT** and **AU** WC base pairs. To verify this hypothesis, we investigated the **GC** base pair focusing on possible electron transfer processes occurring on the $^1n\pi^*$ hypersurface and the associated state crossings. We also considered the WC base pair containing the alternative nucleobase hypoxanthine as a substitute of guanine (**HC** base pair). Hypoxanthine nucleoside (inosine) was recently suggested to be a potential component of primordial versions of RNA.[15] Thus the **HC** base pair

[a] *Department of Physical and Quantum Chemistry, Wroclaw University of Science and Technology, Faculty of Chemistry, Wybrzeże Wyspiańskiego 27, 50-370, Wrocław, Poland. E-mail: robert.gora@pwr.edu.pl*
[b] *Regional Centre of Advanced Technologies and Materials, Faculty of Science, Palacky University, Šlechtitelů 27, 771 46 Olomouc, Czech Republic*
[c] *Institute of Biophysics of the Czech Academy of Sciences, Královopolská 135, 61265 Brno, Czech Republic*
[d] *Institute of Physics, Polish Academy of Sciences, Al. Lotników 32/46, 02-668 Warsaw, Poland. E-mail: szabla@ifpan.edu.pl*

† Electronic supplementary information (ESI) available: Computational details, computed vertical excitation spectra, excited-state PES calculated for the **HC** base pair, description of MD simulations and Cartesian coordinates of key stationary points. See DOI: 10.1039/c9cc06180k

could serve as a valuable reference point to understand the photochemical processes in the **GC** base pair. We performed explorations of the excited-state potential-energy (PE) surfaces of these two base pairs using the algebraic diagrammatic construction to the second order [ADC(2)] method as implemented in the Turbomole 7.3 package.[16]

We started our study with optimizing the ground state geometries of the **GC** and **HC** WC base pairs in the gas phase using the MP2/cc-pVTZ method (see Fig. 1). To separate $^1\pi\pi^*$ and $^1n\pi^*$ excitations we assumed the C_s point-group symmetry corresponding to planar structures. However, analogous optimizations of these base pairs performed without any constraints returned nearly planar geometries as well. Despite only two inter-base hydrogen bonds the **HC** base pair is characterized by a virtually identical orientation of the interacting bases to its biological counterpart **GC**. Slight differences in the common structural motifs are thus the result of the absence of the exocyclic amino group in hypoxanthine and the absence of N–H···O hydrogen bond in **HC**.

The above structural similarities are also reflected by the vertical excitation energies of the LE states presented in Table 1 (obtained at the ADC(2)/cc-pVTZ level). Both **HC** and **GC** are characterized by highly consistent energies and oscillator strengths of low-lying bright $\pi\pi^*$ states, what indicates very similar spectral properties of the two WC base pairs. However, the low-lying $^1\pi\pi^*_{CT}$ state, characterized by an electron transferred from purine to pyrimidine, is significantly destabilized in **HC** (5.91 eV) when compared to **GC** (5.16 eV). This state was attributed to the ultrafast electron-driven proton transfer (EDPT) photodeactivation mechanism in **GC**[7] and we expect that the EDPT process may be unavailable in **HC** at lower excitation energies. This is further supported by the presence of low-lying $^1n\pi^*$ states in the spectrum, due to dipole-forbidden transitions from nonbonding electron pair to π^* orbital, which could have a significant contribution to the photorelaxation of the **HC** base pair.

Based on this initial analysis of vertical excitations it is reasonable to infer that **HC** might indeed be much more vulnerable to photodamage than **GC**. However, we observed one additional and elusive feature of the reactive $^1n\pi^*$ excitations which could have intriguing consequences for the photodeactivation of both considered base pairs. In each case, the lowest energy $^1n\pi^*$ states exhibit partial charge-transfer (CT) character that could be the driving force for yet another deactivation mechanism that was not reported previously. This partial $n\pi^*_{CT}$ character is indicated by 0.17 of e^- charge transferred from carbonyl lone-pair of **G** to π^* orbital localized on **C** and 0.08 of e^- charge transferred from **H** to **C** in the Franck–Condon regions of these base pairs (*i.e.* at their ground-state geometries).

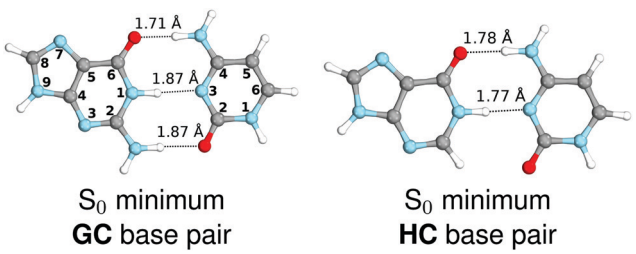

Fig. 1 Ground-state minimum-energy geometries of the **HC** and **GC** base pairs optimized at the MP2/cc-pVTZ level of theory.

Table 1 Selected vertical excitation energies (in eV) of the two considered base pairs, computed using the ADC(2)/cc-pVTZ method, for the ground-state minimum energy structures optimized at the MP2/cc-pVTZ level assuming C_S symmetry (the labels in parentheses denote the symmetric A' and antisymmetric A'' irreducible representations). Complete tables can be found in the ESI

State/transition		E_{exc}/[eV]	f_{osc}	λ/[nm]
GC C_S symmetry				
$S_1(A')$	$\pi\pi^*$	4.86	6.99×10^{-2}	255.3
$S_2(A')$	$\pi\pi^*$	4.91	5.65×10^{-2}	252.7
$S_3(A')$	$\pi\pi^*_{CT}$	5.16	2.84×10^{-2}	240.1
$S_4(A'')$	$n\pi^*_{LE}/n\pi^*_{CT}$	5.37	6.45×10^{-4}	230.9
$S_5(A')$	$\pi\pi^*$	5.37	0.234	230.9
$S_6(A')$	$\pi\pi^*$	5.42	0.407	228.9
HC C_S symmetry				
$S_1(A')$	$\pi\pi^*$	4.809	7.60×10^{-2}	257.8
$S_2(A')$	$\pi\pi^*$	5.044	8.70×10^{-2}	245.8
$S_3(A'')$	$n\pi^*_{LE}/n\pi^*_{CT}$	5.227	2.97×10^{-4}	237.2
$S_4(A')$	$\pi\pi^*$	5.344	0.236	232.0
$S_5(A'')$	$n\pi^*$	5.469	4.24×10^{-4}	226.7
$S_{10}(A')$	$\pi\pi^*_{CT}$	5.912	4.31×10^{-3}	209.7

To further investigate the photoreactivity of the $^1n\pi^*_{CT}$ states, we performed optimizations of S_1 minima, again imposing planar (C_s) symmetry restrictions. The $^1n\pi^*$ state with partial CT character is thus the lowest excited singlet state belonging to the A'' irreducible representation in both **GC** and **HC** base pairs. The corresponding optimized geometries associated with the plateau region on the $n\pi^*_{CT}$ surface are characterized by a substantial increase of the CT character up to 0.57 and 0.52 of e^- for the **GC** and **HC** base pairs, respectively. This partial electron transfer from the purine to the pyrimidine base may also result in a subsequent proton transfer process. In fact, this EDPT mechanism is enabled by significant displacement of the two nucleobases and formation of an excited-state complex (exciplex). The corresponding geometry of the $S_1(n\pi^*_{CT})$ PE minimum can be described as a wobble **GC** base pair with a hydrogen atom transferred photochemically from **G** to **C** (see Fig. 2). Formation of the excited-state wobble base pair is supported by one hydrogen bond and a N···O interaction in which the electron-deficient carbonyl n_O molecular orbital of **G** borrows electron density from the n_N molecular orbital of **C**. The corresponding N···O distance amounts to 2.06 and 2.07 Å in **HC** and **GC**, respectively. The N···O interaction is the key structural feature that enhances charge transfer character of the lowest energy $n\pi^*$ state outside the Franck–Condon region and enables subsequent proton transfer (compare Fig. 2 and 1). Finally, the energy gap separating the S_1 and S_0 states at the $S_1(^1n\pi^*_{CT})$ minima drops below 0.6 eV which indicates that the associated S_1/S_0 state crossings are nearly reached.

The PE profile corresponding to the formation of the wobble geometry and the subsequent EDPT process in **GC** is presented in Fig. 3. This PE profile demonstrates that the wobble exciplex geometry of **GC** can be formed in a barrierless manner upon the population of the lowest energy $^1n\pi^*$ state. This in-plane dislocation of the two bases results in a complete electron transfer from **G** to **C** and drives the base pair towards a plateau on the S_1 PE surface. The subsequent

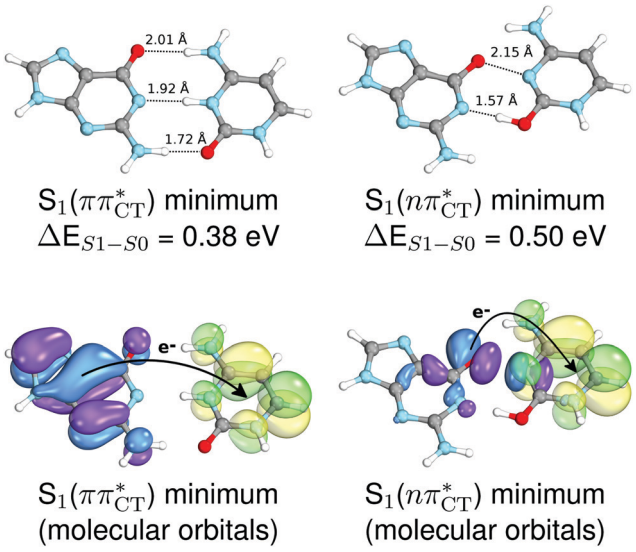

Fig. 2 Minimum-energy geometries of the $^1\pi\pi^*_{CT}$ and $^1n\pi^*_{CT}$ states and the associated occupied (solid blue and violet) and virtual (translucent yellow and green) molecular orbitals.

proton transfer may occur on this plateau and enable the formation of the S_1/S_0 state crossing (conical intersection). Therefore, the EDPT process occurring on the $^1n\pi^*_{CT}$ hypersurface should be considered as a two-stage mechanism, as opposed to one-stage EDPT driven by the $^1\pi\pi^*_{CT}$ state, which was described by Sobolewski and co-workers (see the inset of Fig. 3).[7] The results of our ADC(2) calculations were additionally benchmarked against the SCS-ADC(2) approach and higher level XMS-CASPT2 computations (Section 2.4 in the ESI†). We have also calculated the PE profiles for these two distinct EDPT processes in **HC** (Section 2.3 in the ESI†). The two-stage EDPT process occurring on the $^1n\pi^*_{CT}$ surface of **HC** is virtually identical to what we have already described for **GC**. However, owing to very high excitation energy of the $^1\pi\pi^*_{CT}$ state of **HC** (5.91 eV) the one-stage EDPT process in this base pair could only be triggered at substantially higher excitation energies than in the case of **GC**.

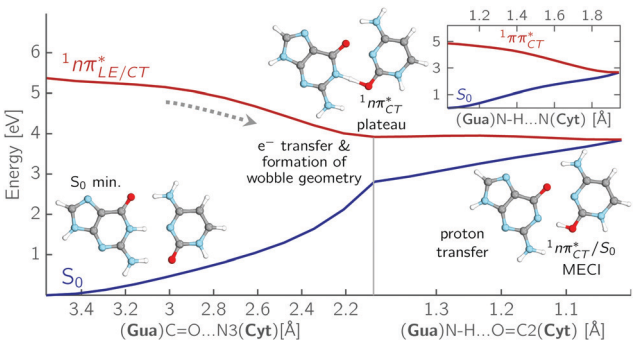

Fig. 3 PE surface cuts illustrating the EDPT mechanism driven by the $^1n\pi^*_{CT}$ state. The PE profile was constructed as a linear interpolation in internal coordinates (LIIC) between the FC region, S_1 plateau and the $^1n\pi^*_{CT}/S_0$ state crossing. The *x* axis in the first part of the profile corresponds to the O···N3 distance, characteristic for the exciplex interaction. The reaction coordinate on the right hand side describes the proton transfer process. The inset shows the one-stage EDPT mechanism triggered on the $^1\pi\pi^*_{CT}$ surface.

It is worth noting that similar $^1n\pi^*_{CT}$ states were also reported in microhydrated cytidine and adenine involving similar state-of-the-art quantum chemical simulations.[13] These examples involved partial electron transfer from a neighbouring water molecule to the chromophore moiety and were also suggested to have a significant contribution to the photochemistry of these molecules in water solution.[13] In the case of the **GC** and **HC** WC base pairs the $^1n\pi^*_{CT}$ state can serve as a photostabilizing deactivation channel. Consequently, once the $^1n\pi^*_{CT}/S_0$ state crossing (shown in Fig. 3) is reached the base pair can repopulate the closed-shell electronic ground-state and the transferred hydrogen atom may be returned to the purine base. This enables barrierless restoration of the canonical structure of the WC base pair.

The excited-state lifetime of the dark $^1n\pi^*$ state in aqueous cytidine was established in several independent experiments which consistently returned the value of ~30 ps.[9] The PE surface shown in Fig. 3 demonstrates that when this dark locally-excited $n\pi^*$ state is populated in **GC** (or **HC**) it may easily acquire a CT character. This CT event could in turn significantly shorten the excited-state lifetime by triggering the highly efficient EDPT mechanism. Interestingly, the population of $^1n\pi^*_{CT}$ states can be facilitated only in the case of the specific hydrogen bonding pattern present in **GC** and **HC**. The formation of an analogous exciplex interaction promoting subsequent proton transfer is not possible in the case of **AT** and **AU** pairs. This could explain why both **T** and **U** are much more susceptible to photodamage in DNA double strands than **C**.

The specific exciplex interaction associated with the $^1n\pi^*_{CT}$ state in **GC** and **HC** is structurally similar to the non-native **GT** wobble pair (see Fig. 4). In each of these cases, the interacting purine and pyrimidine bases are clearly displaced when compared to the native WC pairing pattern, however, crystallographic studies of double-stranded DNA fragments indicate that such displacement should have little or no effect on the sugar-phosphate backbone.[17] To examine this problem more closely we performed an MD simulation of the GGGCCC and GGHCCC B-DNA fragments (including the complementary strands) in which we further mutated one of the **C** bases to a **T** (see Section 2.5 in the ESI†). We simulated 24 and 12 trajectories for the d(GGGTCC)·(GGGCCC) and d(GGGTCC)·(GGHCCC) systems, respectively, assuming different initial conditions. These simulations revealed that the native B-DNA backbone conformation enables very efficient, and practically ultrafast formation of the wobble **GT** interaction after

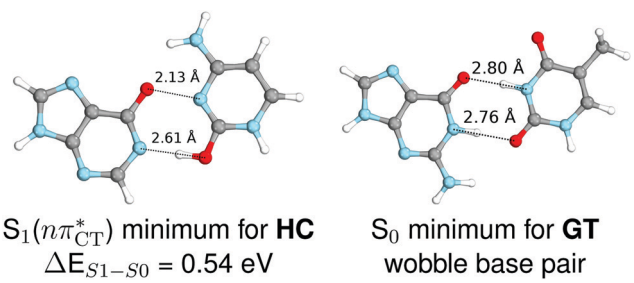

Fig. 4 Comparison of the $S_1(^1n\pi^*_{CT})$ minimum-energy geometry of **HC** and the wobble **GT** base pair in its electronic ground-state. Distances between heteroatoms are marked with dashed lines.

the mutation is introduced. This transition was observed during the first 5 ps in 62.5% of all the trajectories initialized for the d(GGGTCC)·(GGGCCC) system and 75% of the trajectories simulated for the d(GGGTCC)·(GGHCCC) system. Therefore, we anticipate that the timescale of the formation of the wobble $^1n\pi^*_{CT}$ exciplex is likely much shorter than the lifetime of the $^1n\pi^*$ state in cytidine monomer and this process should be easily accessible for **GC** and **HC** in double-stranded DNA.

In conclusion, we demonstrated that long-lived and reactive $^1n\pi^*$ states reported previously as potential sources of photodamage in separate pyrimidine nucleosides may, in fact, facilitate efficient photodeactivation *via* a two-stage electron-driven proton transfer (EDPT) in specific WC base pairs. This channel is enabled by partial charge-transfer character of the $^1n\pi^*$ state and the formation of wobble exciplex geometry. In the case of **GC**, this process could be complementary to the well-documented EDPT photodeactivation mechanism occurring on the $^1\pi\pi^*_{CT}$ hypersurface.[3,7] In contrast, the hydrogen-bonging pattern of **AT** prohibits the formation of the wobble exciplex structure which could stabilize the $^1n\pi^*_{CT}$ character. This may be yet another explanation why the radiationless deactivation involving EDPT is much more favorable in **GC** than in **AT**. Therefore, our findings supplement the rationale behind the substantial photostability of cytosine when compared to thymine and uracil in double-stranded DNA. Our results indicate that this mechanism should be also available in the **HC** base pair containing the non-canonical nucleobase hypoxanthine, which suggests that **HC** could undergo ultrafast photorelaxation despite the apparent inaccessibility of EDPT channel triggered on the $^1\pi\pi^*_{CT}$ PE surface. Presence of such photostabilizing processes in **HC** also reinforces the prebiotic scenarios which involve the formation of the hypoxanthine nucleoside inosine and utilize this molecule in enhancing the rate and fidelity of nonenzymatic RNA template copying.[15] It is worth emphasizing that the EDPT mechanism promoted by dark $^1n\pi^*_{CT}$ states is likely the only ultrafast photorelaxation mechanism available in **HC**. While the primary goal of this preliminary account is to supplement the current knowledge about EDPT and the photoreactivity of dark $^1n\pi^*$ states, more details regarding the role of $^1n\pi^*_{CT}$ exciplexes in WC base pairs could be revealed in the future by pump–probe experiments that could be performed in supersonic expansions or an apolar solvent mimicking the interior of a DNA helix (*e.g.* chloroform). **HC** would be an excellent model system to study this photodeactivation mechanism, since an ultrafast EDPT process triggered in this base pair at lower excitation energies (*e.g.* ~4.8 eV) would most likely originate from the $^1n\pi^*_{CT}$ PE surface.

This work was supported in part by a fellowship from the Simons Foundation (494188 to R. S.), by the Foundation for Polish Science (FNP) and a grant from the National Science Centre Poland (2016/23/B/ST4/01048 to R. W. G.). Support from SYMBIT: European Regional Development Fund [CZ.02.1.01/0.0/0.0/15_003/0000477] is gratefully acknowledged. We thank Mikołaj Janicki and Prof. Andrzej Sobolewski for helpful discussions.

Conflicts of interest

There are no conflicts to declare.

References

1 (*a*) P. Song, Y. Li, F. Ma, T. Pullerits and M. Sun, *Chem. Rev.*, 2016, **16**, 734–753; (*b*) C. T. Middleton, K. D. L. Harpe, C. Su, Y. K. Law, C. E. Crespo-Hernández and B. Kohler, *Annu. Rev. Phys. Chem.*, 2009, **60**, 217–239; (*c*) R. Szabla, H. Kruse, P. Stadlbauer, J. Šponer and A. L. Sobolewski, *Chem. Sci.*, 2018, **9**, 3131–3140; (*d*) J. J. Nogueira, F. Plasser and L. González, *Chem. Sci.*, 2017, **8**, 5682–5691.
2 A. L. Sobolewski and W. Domcke, *Europhys. News*, 2006, **37**, 20–23.
3 T. Schultz, E. Samoylova, W. Radloff, I. V. Hertel, A. L. Sobolewski and W. Domcke, *Science*, 2004, **306**, 1765–1768.
4 (*a*) S. Hammes-Schiffer, *Energy Environ. Sci.*, 2012, **5**, 7696–7703; (*b*) S. Hammes-Schiffer, *J. Am. Chem. Soc.*, 2015, **137**, 8860–8871.
5 (*a*) B. Marchetti, T. N. V. Karsili, M. N. R. Ashfold and W. Domcke, *Phys. Chem. Chem. Phys.*, 2016, **18**, 20007–20027; (*b*) G. Groenhof, L. V. Schäfer, M. Boggio-Pasqua, M. Goette, H. Grubmüller and M. A. Robb, *J. Am. Chem. Soc.*, 2007, **129**, 6812–6819; (*c*) S. Perun, A. L. Sobolewski and W. Domcke, *J. Phys. Chem. A*, 2006, **110**, 9031–9038; (*d*) K. Röttger, H. J. Marroux, A. F. Chemin, E. Elsdon, T. A. Oliver, S. T. Street, A. S. Henderson, M. C. Galan, A. J. Orr-Ewing and G. M. Roberts, *J. Phys. Chem. B*, 2017, **121**, 4448–4455; (*e*) D. Tuna, A. L. Sobolewski and W. Domcke, *J. Phys. Chem. A*, 2014, **118**, 122–127; (*f*) R. Crespo-Otero, A. Mardykov, E. Sanchez-Garcia, W. Sander and M. Barbatti, *Phys. Chem. Chem. Phys.*, 2014, **16**, 18877–18887.
6 (*a*) V. Stert, L. Hesse, H. Lippert, C. Schulz and W. Radloff, *J. Phys. Chem. A*, 2002, **106**, 5051–5053; (*b*) R. Szabla, J. Šponer and R. W. Góra, *J. Phys. Chem. Lett.*, 2015, **6**, 1467–1471; (*c*) J. J. Nogueira, A. Corani, A. El Nahhas, A. Pezzella, M. d'Ischia, L. González and V. Sundström, *J. Phys. Chem. Lett.*, 2017, **8**, 1004–1008; (*d*) M. J. Janicki, R. Szabla, J. Šponer and R. W. Góra, *Faraday Discuss.*, 2018, **212**, 345–358; (*e*) J. Ehrmaier, M. J. Janicki, A. L. Sobolewski and W. Domcke, *Phys. Chem. Chem. Phys.*, 2018, **20**, 14420–14430.
7 (*a*) A. L. Sobolewski and W. Domcke, *Phys. Chem. Chem. Phys.*, 2004, **6**, 2763–2771; (*b*) A. Abo-Riziq, L. Grace, E. Nir, M. Kabelac, P. Hobza and M. S. D. Vries, *Proc. Natl. Acad. Sci. U. S. A.*, 2005, **102**, 20–23; (*c*) A. L. Sobolewski, W. Domcke and C. Hättig, *Proc. Natl. Acad. Sci. U. S. A.*, 2005, **102**, 17903–17906.
8 (*a*) D. B. Bucher, A. Schlueter, T. Carell and W. Zinth, *Angew. Chem., Int. Ed.*, 2014, **53**, 11366–11369; (*b*) K. Röttger, H. J. Marroux, M. P. Grubb, P. M. Coulter, H. Böhnke, A. S. Henderson, M. C. Galan, F. Temps, A. J. Orr-Ewing and G. M. Roberts, *Angew. Chem., Int. Ed.*, 2015, **54**, 14719–14722; (*c*) A. Francés-Monerris, H. Gattuso, D. Roca-Sanjuán, I. Tuñón, M. Marazzi, E. Dumont and A. Monari, *Chem. Sci.*, 2018, **9**, 7902–7911.
9 (*a*) P. M. Hare, C. E. Crespo-Hernández and B. Kohler, *Proc. Natl. Acad. Sci. U. S. A.*, 2007, **104**, 435–440; (*b*) P. M. Keane, M. Wojdyla, G. W. Doorley, G. W. Watson, I. P. Clark, G. M. Greetham, A. W. Parker, M. Towrie, J. M. Kelly and S. J. Quinn, *J. Am. Chem. Soc.*, 2011, **133**, 4212–4215; (*c*) C. Ma, C. C.-W. Cheng, C. T.-L. Chan, R. C.-T. Chan and W.-M. Kwok, *Phys. Chem. Chem. Phys.*, 2015, **17**, 19045–19057; (*d*) A. J. Pepino, J. Segarra-Mart, A. Nenov, I. Rivalta, R. Improta and M. Garavelli, *Phys. Chem. Chem. Phys.*, 2018, **20**, 6877–6890.
10 C. Salet, R. Bensasson and R. Becker, *Photochem. Photobiol.*, 1979, **30**, 325–329.
11 L. Liu, B. M. Pilles, J. Gontcharov, D. B. Bucher and W. Zinth, *J. Phys. Chem. B*, 2016, **120**, 292–298.
12 R. Szabla, J. Campos, J. E. Šponer, J. Šponer, R. W. Góra and J. D. Sutherland, *Chem. Sci.*, 2015, **6**, 2035–2043.
13 (*a*) R. Szabla, H. Kruse, J. Šponer and R. W. Góra, *Phys. Chem. Chem. Phys.*, 2017, **19**, 17531–17537; (*b*) X. Wu, T. N. V. Karsili and W. Domcke, *ChemPhysChem*, 2016, **17**, 1298–1304.
14 S. Mouret, C. Baudouin, M. Charveron, A. Favier, J. Cadet and T. Douki, *Proc. Natl. Acad. Sci. U. S. A.*, 2006, **103**, 13765–13770.
15 (*a*) S. J. Roberts, R. Szabla, Z. R. Todd, S. Stairs, D.-K. Bučar, J. Šponer, D. D. Sasselov and M. W. Powner, *Nat. Commun.*, 2018, **9**, 4073; (*b*) S. C. Kim, D. K. O'Flaherty, L. Zhou, V. S. Lelyveld and J. W. Szostak, *Proc. Natl. Acad. Sci. U. S. A.*, 2018, **115**, 13318–13323.
16 (*a*) C. Hättig, *Advances in Quantum Chemistry*, 2005, vol. 50, pp. 37–60; (*b*) *TURBOMOLE V7.3 2018, a development of University of Karlsruhe and Forschungszentrum Karlsruhe GmbH, 1989–2007*, TURBOMOLE GmbH, since 2007, available from http://www.turbomole.com.
17 O. Kennard, *J. Biomol. Struct. Dyn.*, 1985, **3**, 205–226.

